Synergistic Interaction of Xyloglucan and Xanthan Investigated by Rheology, Differential Scanning Calorimetry, and NMR

Bo-Sook Kim, Makoto Takemasa,* and Katsuyoshi Nishinari*

Department of Food and Human Health Sciences, Osaka City University, 3-3-138 Sugimoto, Sumiyoshi-ku, Osaka 558-8585, Japan

Received September 30, 2005; Revised Manuscript Received January 9, 2006

A new synergistic interaction between tamarind seed xyloglucan and xanthan was found and investigated by rheology, differential scanning calorimetry (DSC), and NMR. The effect of the acetyl and pyruvate groups in the side chain in xanthan on the synergistic interaction was also examined. The shear moduli G' and G'' of the mixture solution of xyloglucan and native (or acetate-free) xanthan increased steeply at around 22 °C upon cooling. An exothermic DSC peak appeared at the same temperature. A drastic decrease in the T_2^* of the acetyl and pyruvate groups of the xanthan side chain was observed from ^{1}H NMR spectra only in the mixture at low temperatures (<25 °C). It was found that the pyruvate group is more restricted in the mixture solution compared with the acetyl group. The mixture of xyloglucan and pyruvate-free xanthan showed no synergistic interaction. We concluded that this synergistic interaction is caused by the intermolecular binding between xyloglucan and xanthan, and, in the heterotypic junction zones, the xanthan side chain becomes a new state that is different from both the coil and helix states.

Introduction

Polysaccharides have been widely used as a food additive to enhance the viscosity and stabilization of products and/or to form a gel. Synergistic combinations of polysaccharides are often employed to manipulate rheological characteristics and to provide effective savings in production costs. The most common systems that show synergistic interaction are the mixtures of xanthan and galactomannan or glucomannan.[1−3] Although the aqueous solution of each polysaccharide alone does not form a gel, xanthan has been reported to form a gel or to increase viscosity by mixing with galactomannans[4,5] or with glucomannans.[6−10]

Xyloglucan alone extracted from tamarind seed also does not form a gel; however, it forms a gel in the presence of a large amount of alcohol or sugar and by the addition of a polyphenol such as epigallocatechin gallate (EGCG),[11] and we recently reported that it forms a synergistic gel by mixing with gellan gum, even under the condition that the concentration of gellan gum is low and not enough to form a gel.[12,13] In this paper, we show a new synergistic interaction between xanthan and tamarind seed xyloglucan. It was also reported that xyloglucan alone can form a gel if a part of the galactose is removed.[14,15]

Xyloglucan is a major structural polysaccharide in the primary cell walls of higher plants.[16] Seeds of the tamarind tree (*Tamarindus indica*) contain xyloglucan as a storage polysaccharide. Tamarind seed xyloglucan is the only xyloglucan that is commercially available at present, and is widely used as a food additive in Japan. The flow behavior of the solution is nearly Newtonian, and very stable against heat, pH, and shear.[17] Xyloglucan is expected to have new applications in food, serving as a thickener and stabilizer, gelling agent, ice crystal stabilizer, and starch modifier.[16,18,19]

The chemical structure of the tamarind seed xyloglucan backbone is β-(1−4)-linked D-glucan, which is the same as that of cellulose. The glucose in the backbone is partially substituted at the O-6 position of glucopyranosyl residues with α-D-xylopyranose. Some of the xylose residues are β-D-galactosylated at O-2. There are three different structures for the repeating units of tamarind seed xyloglucan: heptasaccharide (Glu^4Xyl^3), octasaccharide (Glu^4Xyl^3Gal), and nonasaccharide ($Glu^4Xyl^3Gal^2$).[20]

Xanthan gum is one of the bacterial polysaccharides. Xanthan aqueous solution has a high viscosity, high pseudoplasticity, significant yield stress, and stability, even at low concentrations over wide pH, temperature, and salt content ranges.[21] The main chain consists of β-D-(1,4)-linked glucose, which is the same as cellulose. A trisaccharide side chain, consisting of α-D-mannose, β-D-glucuronic acid, and β-D-mannose is attached to every second glucose residue of the main chain.[22] The one mannose residue is connected to the backbone, and is partially acetylated. Parts of the terminal mannose residues are pyruvated to some extent, depending on the *Xanthomonas campestris* substrain.[23] Xanthan undergoes a temperature-induced conformational transition.[24,25] This coil−helix transition is affected by the addition of salt and the charge density of xanthan related to the side-chain chemical structure. Correlations between the acetyl and the pyruvate contents and the midpoint temperature of the transition have been reported.[26−29]

Up to the present, synergistic interactions of mixtures for various kinds of polysaccharides have been studied, not only for application in industries, such as making a new texture in food and industrial products, but also for more fundamental purposes, such as investigating the intermolecular interaction between different polysaccharides. Several combinations of two polysaccharides showing synergistic interactions are known, such as xanthan/galactomannan or konjac glucomannan (KM), carrageenan/galactomannan or KM, and agarose/carrageenan.[30−32] Morris pointed out that two common features of these systems are that one of the two polysaccharides consists of a β-(1−4)-linked backbone, and the other undergoes a thermoreversible

* Corresponding authors. Tel: +81-6-6605-2818. Fax: +81-6-6605-3086. E-mail: takemasa@physics.soft-matter.org (M.T.); nisinari@life.osaka-cu.ac.jp (K.N.).

10.1021/bm050734+ CCC: $33.50
Published on Web 03/22/2006

disorder−order (coil−helix) transition.[33] Xanthan/xyloglucan, which will be shown in this paper along with the above-mentioned combinations, and gellan gum/xyloglucan also lie on these common features. This similarity hints to the same interaction mechanism. However, the origin of this interaction and the reason these combinations are so special have been controversial, and it is still difficult to understand the detailed mechanism of the synergistic interaction of the polysaccharide mixture. For instance, the xanthan/galactomannan mixture, which is one of the most extensively studied mixtures, has been investigated more than 30 years, but even the most important and basic question of whether two polysaccharides form a heterotypic junction zone has been still in dispute. It is necessary to perform systematic measurements for these systems and for new systems.

We found that the mixing of xyloglucan and xanthan results in an increase in the elastic moduli, and this is a synergistic interaction, which is also the combination of the helix-forming polysaccharide and β-D-(1−4)-linked cellulosic polysaccharide. The effect of the acetyl and pyruvate groups in the side chain of xanthan on the synergistic interaction of the mixture of xyloglucan and xanthan has been investigated by dynamic viscoelasticity, differential scanning calorimetry (DSC), and nuclear magnetic resonance (NMR) to clarify the details of the synergistic interaction. Since this kind of synergistic interaction is not so common, and appears only for the specific combinations of polysaccharides with specific chemical structure, the investigation of this new interaction will also be helpful to accumulate knowledge for establishing a generic model of the synergistic interaction, and to control the physicochemical properties of the aqueous solutions of polysaccharides.

Experimental Section

Materials. Xyloglucan extracted from tamarind seed was a gift provided from Dainippon Pharmaceutical Co., Ltd. (Osaka, Japan). Xyloglucan was precipitated with acetone to remove insoluble substances.

Three different xanthans were used to clarify the effect of the chemical structure of xanthan on the synergistic interaction. Three types of xanthan, a native xanthan, which has both acetyl and pyruvate groups, an acetate-free xanthan, and a pyruvate-free xanthan, were kindly supplied by CP Kelco (U.S.A.), and were used without further purification.

To make mixed solutions, aqueous solutions of xyloglucan alone and xanthan alone were prepared at 1.0 wt % by dispersing each powder in distilled water for 12 h at room temperature. Then, these two solutions of the same weight were mixed. The total polysaccharide concentration of the mixed solution was fixed at 1.0 wt % for all the mixed solutions.

Methods. *Rheological Measurements*. Dynamic viscoelastic measurements were carried out using a Rheostress 600 (Haake, Thermo Electron, Germany) with a cone plate geometry (diameter, 59.997 mm; gap, 0.103 mm; cone angle, 1.995°). The exposed surface of the sample was covered with silicone oil to avoid evaporation of water in the solution, immediately after the sample solution was set on the lower plate. The temperature dependence of the storage (G') and the loss (G'') shear moduli was examined at a rate of 0.5 °C/min and at an angular frequency of 1.0 rad/s. For the rheological and the DSC measurements, at first, a heating measurement was performed, then a subsequent cooling, and next a reheating measurement was done.

DSC Measurements. DSC measurements were carried out by using a high-sensitivity calorimeter, Micro DSC III (Setaram, France). Exactly the same amount (800 ± 5 mg) of the sample (polysaccharide aqueous solutions) and reference (distilled water) solutions were put into the DSC cell, and then placed in the calorimeter. The scan rate was fixed at 0.5 °C/min.

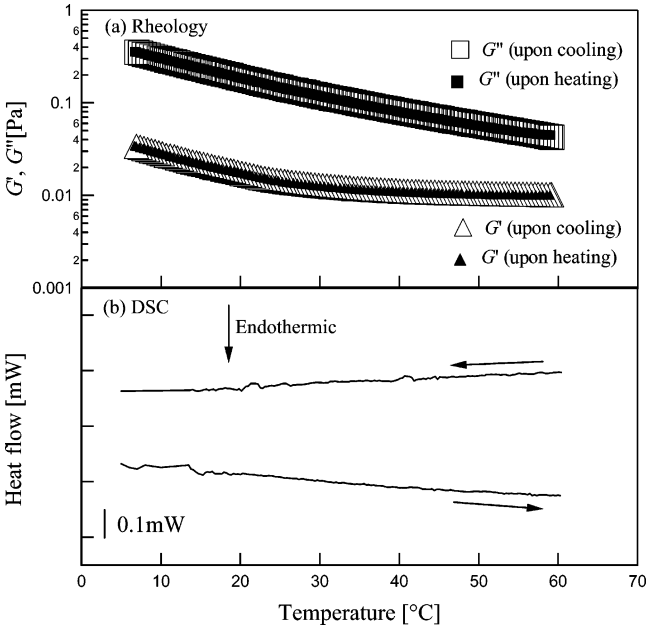

Figure 1. (a) Temperature dependence of storage modulus, G', and loss modulus, G'', and (b) DSC curves upon cooling and subsequent heating for a 1.0 wt % xyloglucan solution. The scanning rate is 0.5 °C/min, and the angular frequency is 1.0 rad/s.

NMR Measurements. ^{1}H NMR spectra were obtained with UnityPlus500 (B_0 = 11.7 T) (Varian, U.S.A.) to elucidate the mechanism of the synergistic interaction for the xyloglucan/xanthan mixture in 99.9% D_2O at the molecular level. Sodium 2,2-dimethyl-2-silapentane-5-sulfonate (DSS) was also added as the inner standard of the chemical shift. It was confirmed that the peak attributed to the acetyl group was not observed for acetate-free xanthan at all, and the peak attributed to the pyruvate group was not observed for pyruvate-free xanthan. The apparent transverse relaxation time, T_2^*, was estimated from the observed line width, ν, of the peak by an equation,

$$T_2^* = \frac{1}{\pi\nu}$$

The NMR spectra were measured at a constant temperature. To obtain the temperature dependence of the spectra and the T_2^*, the temperature was raised stepwise in increments of 5 °C. Each interval for the temperature raise was 30 min. The temperature was stabilized during this time, and the spectrum was recorded.

Results and Discussion

Rheological and thermal behaviors of xyloglucan and xanthan alone were examined before the measurements of their mixture. Figure 1 shows the temperature dependence of the dynamic shear moduli (Figure 1a) and the DSC curves (Figure 1b) for a 1.0 wt % aqueous solution of xyloglucan alone. Both the storage modulus, G', and the loss modulus, G'', increased monotonically with decreasing temperature in the entire temperature range. No DSC peak was found. Both the rheological and DSC results shown here are in good agreement with previous findings that there is no characteristic structural change for xyloglucan[15] such as the coil−helix conformational transition observed for xanthan.

Figure 2 shows DSC cooling curves for 0.5 and 2.0 wt % aqueous solutions of three types of xanthan: a native xanthan, an acetate-free xanthan, and a pyruvate-free xanthan. Since the xanthan concentration in the mixtures of xyloglucan and xanthan used is fixed at 0.5 wt %, the DSC measurement was carried out at the same concentration. The aqueous solutions of 2.0 wt

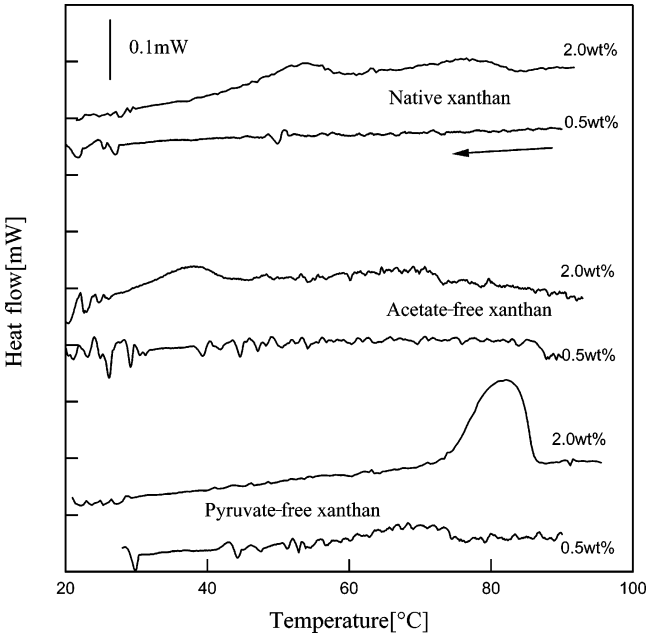

Figure 2. DSC cooling curves for 0.5 and 2.0 wt % native xanthan, acetate-free xanthan, and pyruvate-free xanthan. The cooling rate is 0.5 °C/min.

% xanthan with different chemical structures—a native xanthan, an acetate-free xanthan, and a pyruvate-free xanthan—showed an exothermic peak upon cooling at 53, 37, and 81 °C, respectively. The DSC peak of xanthan was attributed to the conformational change from helix to coil (upon heating, not shown) and from coil to helix (upon cooling), respectively.[34] It is known that acetate-free xanthan has a lower stability of the helix structure, and the helix−coil transition temperature is lower than that of a native xanthan aqueous solution. On the other hand, the coil−helix transition temperature of pyruvate-free xanthan is higher than that of native xanthan because of the higher stability of the helix. For the result of 0.5 wt % xanthan, the peak of 0.5 wt % pyruvate-free xanthan appeared at 69 °C, which is 12 °C lower than that of 2.0 wt %. It was well-established that the total concentration of the cation is responsible for the coil−helix transition temperature, and the polymer concentration is not essential[35] for the coil−helix transition of negatively charged polysaccharides, such as κ-carrageenan,[36] gellan gum,[37] and xanthan.[38] Hence, this peak shift is caused by the decrease in the activity coefficient of the counterion accompanied by the decrease in the polymer concentration. In the cases of 0.5 wt % native xanthan and 0.5 wt % acetate-free xanthan, no reliable DSC peak was detected. These seem to be due to a sensitivity limit of the apparatus, because it was reported that, even at lower concentrations, xanthan undergoes the coil−helix transition,[39] and the transition enthalpies for 2.0 wt % native xanthan and acetate-free xanthan are much smaller than that for 2.0 wt % pyruvate-free xanthan. By using the relation between the total activity coefficient and the coil−helix transition temperature,[39,40] the coil−helix transition temperature can be estimated as $T_{CH} = 33$ and 20 °C for native and acetate-free xanthan, respectively. That is, 0.5% aqueous solutions of native and acetate-free xanthan also undergo the coil−helix conformational transition.

Figure 3 shows (a) cooling and (b) heating DSC curves for 1.0 wt % mixtures of xyloglucan/native xanthan, xyloglucan/acetate-free xanthan, and xyloglucan/pyruvate-free xanthan. For all the solutions, an exothermic peak and an endothermic peak were observed upon cooling and heating, respectively. Almost no thermal hysteresis was observed for the three mixture solutions. For the mixtures of xyloglucan/native xanthan and xyloglucan/acetate-free xanthan, DSC exothermic peaks were observed at 18 and 20 °C upon cooling, respectively. It is noteworthy that the DSC peak temperature of the mixture with acetate-free xanthan is higher than that with native xanthan, but, for the aqueous solutions of xanthan alone, the peak temperature for acetate-free xanthan is lower than that for native xanthan, as shown in Figure 2. This suggests that the DSC peaks of the mixture solutions originate not from the coil−helix transition, but from the synergistic interaction. However, the peak temperature for the mixture of xyloglucan/pyruvate-free xanthan, at about 70 °C, was much higher than those for the other two mixtures. The peaks observed for the mixtures of xyloglucan/native xanthan and xyloglucan/acetate-free xanthan are caused by the synergistic interaction between xyloglucan and xanthan, because no peak could be observed from the solutions of each component (1 wt % xyloglucan as shown in Figure 1, and 0.5 wt % native xanthan and 0.5 wt % acetate-free xanthan as shown in Figure 2).

At this point, the detailed origin of this DSC peak is not clear, but we can expect only a few origins for the characteristic behavior of the heat flow: (1) the conformational change of xanthan, such as the coil−helix transition, (2) the self-aggregation of each component, and/or (3) the direct interaction between xanthan and xyloglucan. Even in the case of scenario 1, we can safely say that the addition of xyloglucan causes a huge increase in the transition enthalpy, and this is also classified into a kind of synergistic interaction.

DSC transition enthalpies, ΔH, estimated from the DSC peak area for the conformational transition from coil to helix (or helix to coil) of three xanthan solutions—native, acetate-free, and pyruvate-free xanthan—are ~2.6, 2.6, and 11.4 J/g, respectively. The values of ΔH for the three mixture solutions, which were estimated on the basis of the mass of one solute (xanthan or xyloglucan), were ~5.5, 16.2, and 9.4 J/g, respectively. The reported values for other synergistic interactions are 2−24 J/g, depending on the salt condition for xanthan/galactomannan,[41] 20 J/g for native xanthan/glucomannan, 30 J/g for acetate-free xanthan/glucomannan,[9] and 4−18 J/g for xyloglucan/EGCG.[11]

Figure 4a shows the temperature dependence of G' and G'' for 0.5 wt % native xanthan and 0.5 wt % xyloglucan alone, and a 1.0 wt % mixture observed upon cooling. For the mixture solution, both G' and G'' increased steeply at around 22 °C with decreasing temperature. Upon subsequent heating, both values showed a steep decrease at the same temperature (see inset). There is almost no thermal hysteresis.

Additionally, the temperature at which G' and G'' steeply increased corresponds to the DSC peak temperature. This strongly suggests that the large increase in the shear moduli has the same origin as the DSC peak, and it clearly means that this steep change of G' and G'' is caused by the mixing of xyloglucan and native xanthan, and is the result of a synergistic interaction. The transition temperature and storage and loss moduli for the mixture of xyloglucan and acetate-free xanthan are similar to those of the mixture of xyloglucan with native xanthan, particularly for the temperature at which G' increased steeply upon cooling (Figure 4b) and the DSC peak temperature (Figure 3). However, the mixture with pyruvate-free xanthan showed an essentially different behavior. The G' and G'' of the 1 wt % mixture solution of xyloglucan and pyruvate-free xanthan are almost the same as those of 0.5 wt % pyruvate-free xanthan alone, as shown in Figure 4c. Moreover, the temperature at which G' and G'' remarkably increased upon

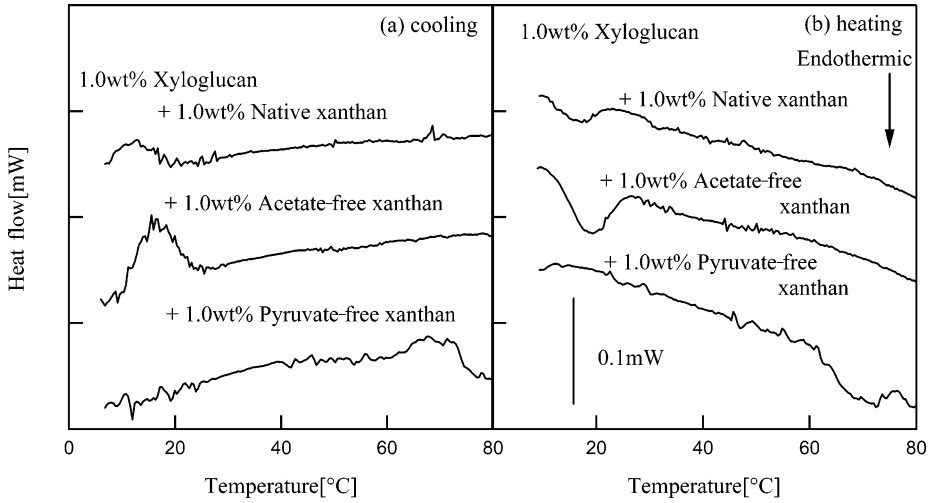

Figure 3. DSC curves of xyloglucan/native xanthan, xyloglucan/acetate-free xanthan, and xyloglucan/pyruvate-free xanthan upon (a) cooling and (b) subsequent heating. The scanning rate is 0.5 °C/min.

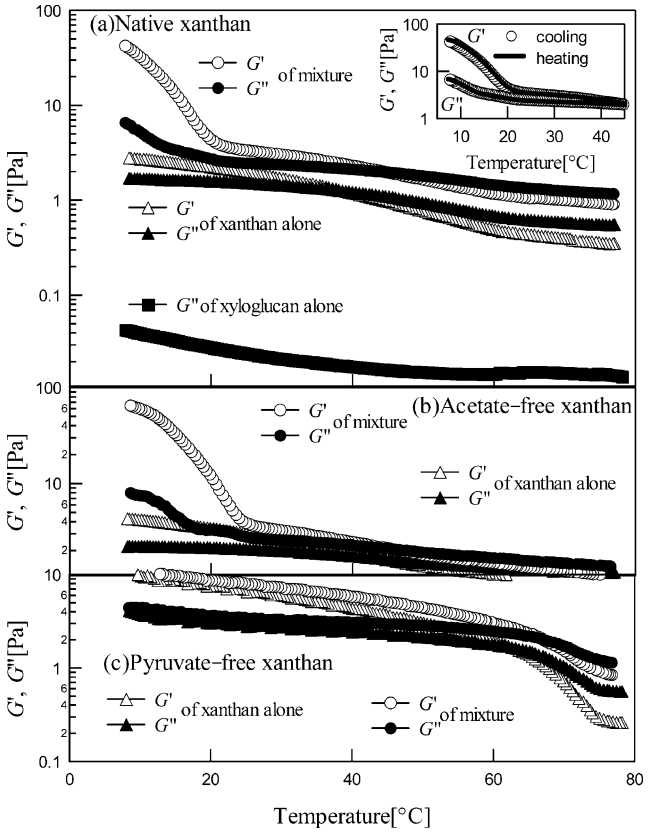

Figure 4. (a) Temperature dependence of the G′ and G″ of 0.5 wt % xyloglucan alone, 0.5 wt % native xanthan alone, and a 1.0 wt % mixture of xyloglucan/native xanthan (weight ratio = 1:1); (b) that of 0.5 wt % acetate-free xanthan alone and a 1.0 wt % mixture of xyloglucan/acetate-free xanthan (weight ratio = 1:1); and (c) that of 0.5 wt % pyruvate-free xanthan alone and a 1.0 wt % mixture of xyloglucan/pyruvate-free xanthan (weight ratio = 1:1) upon cooling. The cooling rate is 0.5 °C/min, and the angular frequency is 1.0 rad/s. The inset in panel a represents the cooling and subsequent heating curves of the mixture with native xanthan. Although the G' of xyloglucan alone could not be observed because of the limitation of the sensitivity, $G' < G''$.

cooling for the mixture is the same as that for pyruvate-free xanthan alone. These results indicate that native xanthan and acetate-free xanthan form a thermoreversible gellike structure by mixing with xyloglucan at low temperatures, but pyruvate-free xanthan does not.

From the spectroscopic aspects of the rheology on this mixture system, as shown in Figure 5, it is also found that the network structure that induces a gellike behavior is formed at low temperatures for the mixtures of xyloglucan with native xanthan or acetate-free xanthan, and, as for the mixture with pyruvate-free xanthan, no essential difference was observed compared with the aqueous solution of pyruvate-free xanthan alone.

The two mixture solutions at 5 °C of Figure 5a—the mixtures of xyloglucan/native xanthan and xyloglucan/acetate-free xanthan—showed the typical gellike frequency dependence, and $G' > G''$ in the entire frequency region from 0.1 to 100 rad/s, and tan $\delta \leq 0.1$. In contrast, the mixture solution with pyruvate-free xanthan showed essentially different behavior from that of the other two mixture solutions. That is, $G' > G''$ in the entire frequency region, but G' showed a larger frequency dependence compared with those for the above-mentioned two mixture solutions, and tan $\delta \geq 0.5$. It means that the mixture with pyruvate-free xanthan is more liquid-like compared with the mixtures with native xanthan or acetate-free xanthan. It shows the same frequency dependence as that for pyruvate-free xanthan alone, and it is a typical frequency dependence of the so-called *weak gel* system. Additionally, the mixtures with native xanthan and acetate-free xanthan at both 40 °C and 5 °C showed different behaviors, while the mixture with pyruvate-free xanthan and the aqueous solution of pyruvate-free xanthan alone showed basically the same behavior at both temperatures. This is consistent with the result of the temperature dependence of G' and G'' described before, and supports the fact that, at low temperatures, native xanthan and acetate-free xanthan show the synergistic interaction by mixing with xyloglucan, but the pyruvate-free xanthan does not interact with xyloglucan. The values of G' at 40 °C for the mixture with pyruvate-free xanthan and pyruvate-free xanthan alone are higher than those of the other solutions. It is envisaged that the conformational difference in xanthan affects the values of moduli, because at 40 °C, pyruvate-free xanthan is in the helix state, which can be confirmed from the DSC results of Figure 2.

At high temperatures such as 80 °C (Figure 5c), all the solutions, both the mixture solutions and the aqueous solutions of xanthan alone, showed essentially the same behavior. A crossover of G' and G'' was observed, and $G'' > G'$ at low frequencies. The slopes of G' and G'' were slightly smaller than 2 and 1, respectively. This means that the relaxation time is distributed even at high temperatures, but is normally an observed behavior for polymer solutions at semidilute regions,

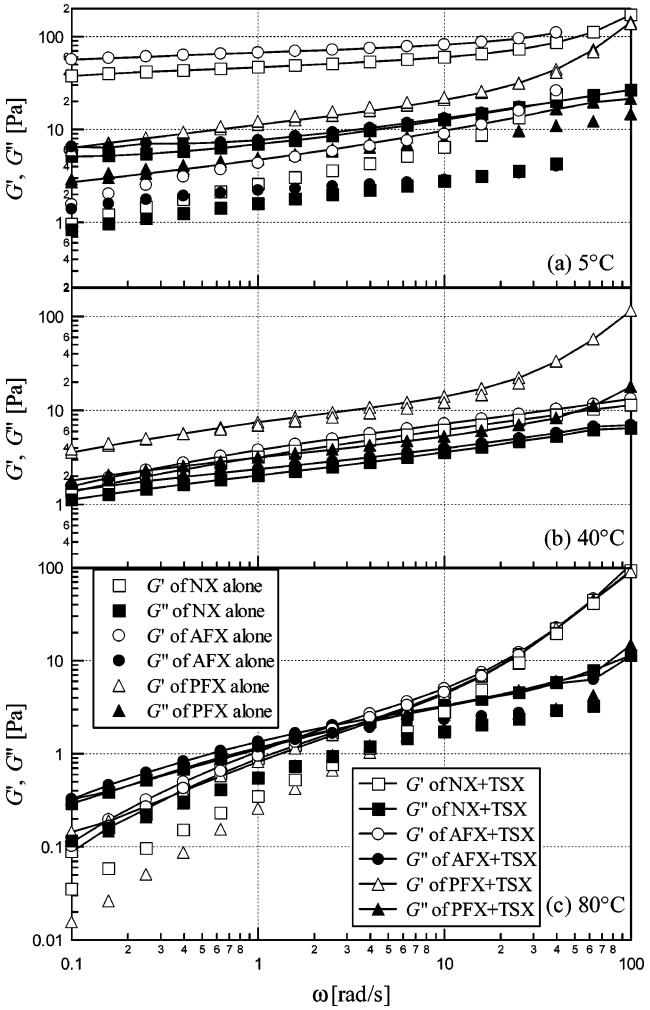

Figure 5. Frequency dependence of G' and G'' for 1.0 wt % mixtures of xyloglucan and native xanthan, acetate-free xanthan, and pyruvate-free xanthan (weight ratio = 1:1) at (a) 5 °C, (b) 40 °C, and (c) 80 °C. The open and filled symbols represent G' and G'', respectively. The abbreviation in the figures, TSX, NX, AFX, and PFX represent tamarind seed xyloglucan, native xanthan, acetate-free xanthan, and pyruvate-free xanthan, respectively. The concentration of the aqueous solution of xanthan alone is 0.5 wt %, and the concentrations of each polysaccharide in the mixture are the same (total polysaccharide concentration, 1.0%).

probably caused by the polydispersity of the molar mass and the above-mentioned tenuous association.

The mechanical spectra observed for the mixture solutions at temperatures higher than 40 °C were almost the same as those for the solutions of xanthan alone, one component of the solute in the mixture. Hence, the suggestions from the frequency dependence of G' and G'' observed at different temperatures that (1) the rheological behavior is dominated mainly by xanthan at 40 and 80 °C, and (2) there is no synergistic interaction between xanthan and xyloglucan, are also supported by the mechanical spectra.

From the viewpoint of the appearance of the DSC peak, the mixture solutions with xanthan containing a pyruvate group showed basically similar results. In contrast, the mixture with pyruvate-free xanthan is much different from other mixtures, which suggests that pyruvate-free xanthan did not interact with xyloglucan in the same way. Both the mixture of xyloglucan with pyruvate-free xanthan and pyruvate-free xanthan alone showed the endothermic peak at the same temperature upon heating, as shown in Figure 6. The transition enthalpy estimated

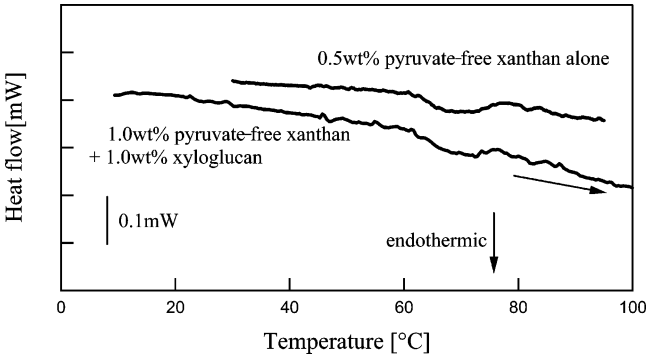

Figure 6. Heating DSC curves for 1.0 wt % mixture of xyloglucan and pyruvate-free xanthan (weight ratio = 1:1) and 0.5 wt % pyruvate-free xanthan alone. The scanning rate is 0.5 °C/min.

from the DSC peak area of the mixture was almost the same as that of pyruvate-free xanthan alone. Therefore, it directly means that no synergistic interaction occurs for the mixture of xyloglucan and pyruvate-free xanthan in terms of DSC, and also indicates that the pyruvate group is essential for the synergistic interaction between xanthan and xyloglucan.

To confirm the role of the pyruvate group in more detail, we performed NMR experiments. Figure 7 shows the ^{1}H spectra of the mixture of native xanthan and degraded xyloglucan recorded at various temperatures. The peak observed at 2.17 ppm is attributed to the acetyl group, and that observed at 1.45 ppm is attributed to the pyruvate group.[42−44] Peaks of the acetyl and pyruvate groups became broader with decreasing temperature. The peaks became much broader around 25 °C, but the peak position (chemical shift) was not changed (<0.01 ppm). This indicates that the motion of the acetyl and pyruvate groups becomes restricted around 25 °C, and the correlation time increased with decreasing temperature. The fact that these peaks became broader does not directly mean an intermolecular binding between xyloglucan and the acetyl and/or pyruvate groups in the side chain of xanthan, although the increase in the macroscopic viscosity is probably related to the increase in the microscopic viscosity for the polymer with large molar masses and correlation time, as expected from the rheological measurements.

To evaluate the motion of the proton attributed to each peak separated from the viscosity effects, the apparent transverse relaxation time, T_2^*, was estimated from each peak. As shown in Figure 8, the T_2^* of the acetyl and pyruvate peaks in xanthan and the anomeric proton, H-1, of the galactose in xyloglucan at various temperatures was estimated to compare the mobility of these groups in the xanthan side chain with those of the other peaks. The T_2^* of the peaks for the acetyl and pyruvate groups in the mixture of degraded xyloglucan and native xanthan decreased steeply at around 25 °C upon cooling. This characteristic temperature is almost the same as that observed in rheological and DSC measurements. At temperatures below 20 °C, the NMR peak attributed to the acetyl group became broader, but can still be detected, while the pyruvate peak was not detectable at low temperatures. This decrease in T_2^* indicates that the mobility of the pyruvate group located at the terminal mannose of the xanthan side chain is more affected by the addition of xyloglucan, compared to that of the acetyl group. The peaks of the pyruvate and acetyl groups in xanthan alone also gradually became broader with decreasing temperature. However, the T_2^* of the acetyl group in pyruvate-free xanthan did not exhibit such a steep decrease in the entire temperature range investigated. These results clearly showed that a syner-

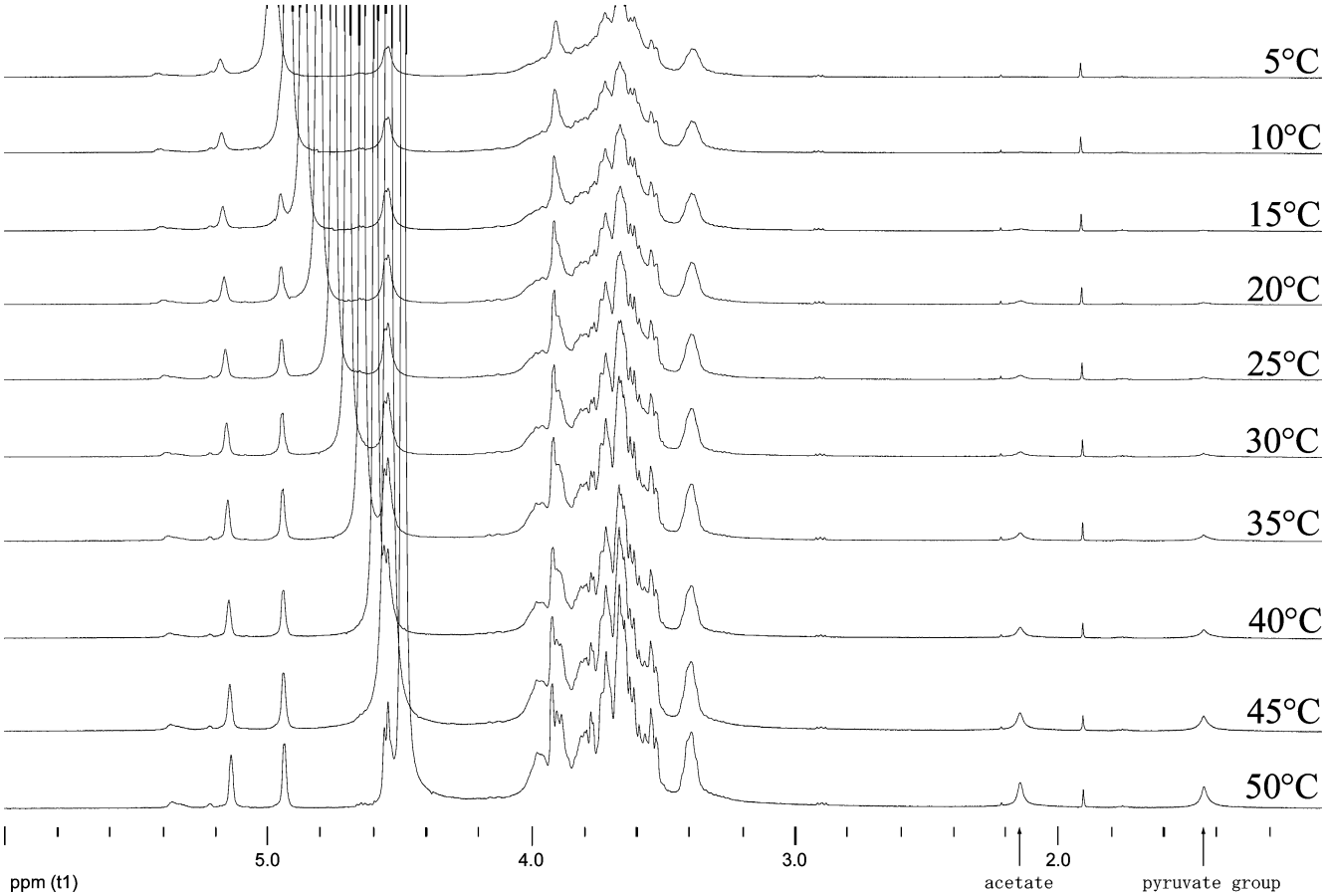

Figure 7. Temperature dependence of the 1-H spectrum for the mixture of native xanthan and degraded xyloglucan. The peak observed at 2.17 ppm is attributed to the acetyl group, and that at 1.45 ppm is attributed to the pyruvate group, as shown by the arrows at the bottom of the figure. The large and temperature-dependent peak observed at 4.5−5.0 is attributed to HDO.

gistic interaction occurred by the addition of xyloglucan, and a motional restriction of the side chain in xanthan occurred, which was not observed for xanthan alone.

The T_2^* of methyl protons in the acetate and pyruvate groups of the aqueous solution of native xanthan alone gradually decreased, even at temperatures lower than the coil−helix transition temperature, and their values of T_2^* are almost the same. The T_2^* of the pyruvate group is slightly smaller than that of the acetate group, which is probably caused by the different flexibilities in the linkage. The pyruvate substituents of xanthan are attached more rigidly to the terminal mannose residue of the trisaccharide side chain (as a 4,6-ketal ring), compared with the acetate substituents attached to the inner mannose. As mentioned before, a 0.5 wt % xanthan solution also undergoes the conformational transition. At temperatures lower than the estimated coil−helix transition temperature, T_2^* was not changed as much as that in the coil state at higher temperatures. On the other hand, their T_2^* values in the presence of xyloglucan drastically decreased at temperatures lower than the temperature at which the synergistic interaction appeared.

The experimental finding that the effect of the synergistic interaction on the mobility of the xanthan side chain is larger than that of the coil−helix transition means that the side chain of xanthan is restricted at low temperatures in the mixture solution, and that the state of the side chain in the mixture at low temperatures is different from both that in the coil state of xanthan and that in the helix state.

Although, even for the most extensively studied system showing synergistic interaction, the xanthan/galactomannan

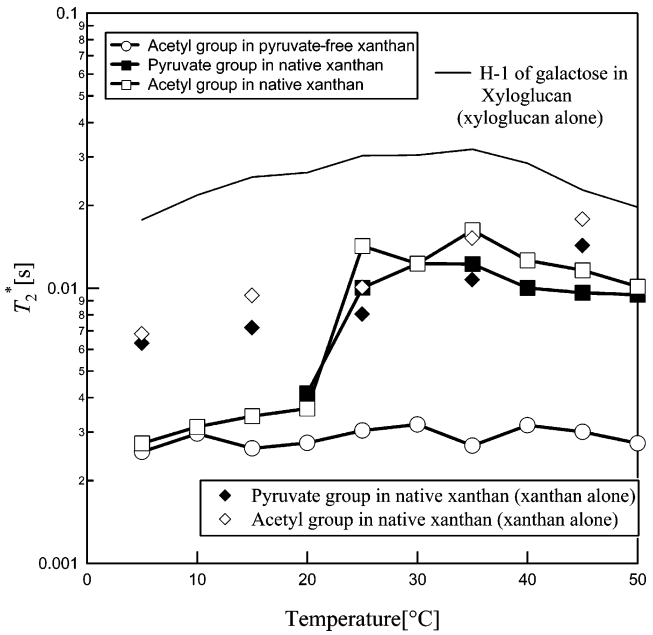

Figure 8. Temperature dependence of the T_2^* of the acetyl and pyruvate groups located at the end of the side group of xanthan in aqueous solutions of xanthan alone, xyloglucan alone, and in xyloglucan/xanthan mixture solutions. The T_2^* of the pyruvate group in the mixture solution with native xanthan could not be estimated at low temperatures because the peak disappeared. The T_2^* of the anomeric proton H-1 of the galactose in xyloglucan is also shown for comparison.

mixture, the binding site has still not been clear and in dispute, here we consider the model for the synergistic interaction of the xyloglucan/xanthan mixture in comparison to the xanthan/galactomannan mixture system. A straightforward model of the origin of this synergistic interaction is a formation of heterotypic junction zones of xanthan and xyloglucan, and the binding site in xanthan is a pyruvate group. It has also been reported that the lack of pyruvate group[45] and the lack of terminal mannose[46] in the side chain of xanthan inhibits the synergistic interaction for xanthan/galactomannan systems. However, these results do not directly indicate that the pyruvate group is the binding site. Both depyruvated xanthan and xanthan without terminal mannose show essentially the same coil−helix transition, but the transition temperature is higher than that for native xanthan. This means that the structure of the helix for these samples is more stable. It is suggested that the synergistic interaction between xanthan and galactomannan occurs with the helix part of xanthan, and the heterotypic structure then reverts to a new heterotypic junction zone,[47] and it becomes difficult for the heterotypic junction zones to be formed if the helix conformation is stable compared to the heterotypic junction zones. This model can explain why the deacetylation of xanthan promotes the synergistic interaction, because the deacetylation makes the helical conformation more unstable, as can also be seen in Figure 2, even if the pyruvate group is not a binding site for xanthan.

By using X-ray diffraction, Morris and co-workers succeeded in obtaining a new pattern that appeared only in the mixture, clearly indicating that heterotypic junction zones can be formed at least in the highly concentrated, almost solid state.[48] Although, the obtained diffraction patterns were not clear enough to establish a complete molecular model. In the case of a xanthan/guar gum mixture, even with the nonassociating phases of xanthan and guar gum, it can also explain the obtained diffraction pattern.[49]

A better and clearer pattern was obtained for acetan and glucomannan.[50] These results suggested that the glucomannan molecule adopted the helical conformation in a "hybrid helix" structure, a xanthan and glucomannan double helix. Chandrasekaran et al. reported that there are no restrictions within the acetan/glucomannan double helix for replacing the glucomannan with a galactomannan. Even though this model is correct for xanthan/galacto- and glucomannan mixtures, the backbone structure of xyloglucan is essentially different from the glucomannan molecule, and the side chain structure is also different. Therefore, whether xyloglucan can adopt a 6-fold, left-handed, parallel double helix of 55.4 Å pitch with xanthan is not clear and depends on both the cellulose backbone and the galactose substitution patterns.

Tako et al. proposed that the side chain of xanthan has an essential role on the synergistic interaction of xanthan/galactomannan, the so-called "lock and key" model.[45,51] However, as Morris pointed out,[33] this model appears to have little basis in experimental evidence and incorporates some implausible features. Furthermore, the specific groups on the galactomannan molecules have an essential role in this model, and strongly depend on the chemical structure of galactomannan, and it is difficult to apply this model to the synergistic interaction of the xanthan/xyloglucan mixture, whose structure is essentially different.

The transition temperature and the other characteristic properties of the mixture with deacetylated xanthan were almost the same as that with native xanthan, which suggests that the mechanism of the formation of heterotypic junction zones is different from that for the xanthan/galactomannan mixture. Furthermore, according to Richter et al., for xanthan/galactomannan mixtures, no significant change in the line width of the pyruvate group in xanthan was observed.[52] In contrast, it was found that there was drastic line broadening, and that the pyruvate group was more restricted at low temperatures in the presence of the synergistic interaction. Hence, the detailed mechanism of the synergistic interaction between xanthan/xyloglucan may be different from that between xanthan/galacto- and/or glucomannan, but it is safe to say that, even in this mixture system (the xanthan and xyloglucan mixture), the conformation of xanthan is changed into a new one at low temperatures by mixing with xyloglucan, because such a drastic line broadening was not observed for the aqueous solutions of xanthan alone. This strongly suggests that the heterotypic junction zone is formed.

Conclusion

A new synergistic interaction was found for the aqueous solution of the mixture of tamarind seed xyloglucan and native xanthan. By mixing xanthan and xyloglucan, the system exhibits thermoreversible physical gellike properties at low temperatures. A steep increase in both the storage and loss shear moduli was observed around 22 °C upon cooling, and a conspicuous exothermic DSC peak appeared at the same temperature, although these characteristic behaviors did not appear for the aqueous solution of each component alone. The effect of acetyl and pyruvate groups in the xanthan side chain on this synergistic interaction was also investigated. The mixture of xyloglucan and acetate-free xanthan showed essentially the same synergistic interaction as that with native xanthan, but the lack of a pyruvate group inhibits the synergistic interaction. This indicates that the pyruvate group substituted at the terminal mannose of the xanthan side chain plays a key role in this synergistic interaction. The line width of the ^{1}H NMR results showed a drastic restriction in the xanthan side chain, which was not observed even in the helix state of xanthan alone. This suggests that the xanthan side chain becomes a new state that is different from the coil and helix states.

Acknowledgment. We thank Mayumi Shirakawa, Kazuhiko Yamatoya (Dainippon Pharmaceutical Co. Ltd., Japan), and Neil Morrison (CP Kelco, San Diego, CA) for providing us with the samples of tamarind seed xyloglucan and xanthan with different chemical structures, respectively. This work was partly supported by the Osaka City University Priority Research Project. BS.K. and M.T. thank the Japanese Ministry of Education, Culture, Sports, Science and Technology for financial support for foreign students and JSPS research fellowships for young scientists, respectively.

References and Notes

(1) Morris, E. R. In *Food Gels*; Harris, P., Ed.; Elsevier Science Publishers: New York, 1990; pp 291−359.
(2) Morris, V. J. In *Functional Properties of Food Macromolecules*; Hill, S. E., Ledward, D. A., Mitchell, J. R., Eds.; Kluwer Academic Publishers: Norwell, MA, 1998; pp 143−226.
(3) Williams, P. A.; Phillips, G. O. In *Food Polysaccharides and Their Applications*; Stephen, A. M., Ed.; Marcel Dekker: New York, 1995; pp 463−500.
(4) Morris, E. R.; Foster, T. J. *Carbohydr. Polym.* **1994**, *23*, 133−135.
(5) Dea, I. C. M.; Morris, E. R.; Rees, D. A.; Welsh, E. J.; Barnes, H. A.; Price, J. *Carbohydr. Res.* **1977**, *57*, 249−272.
(6) Brownsey, G. J.; Cairns, P.; Miles, M. J.; Morris, V. J. *Carbohydr. Res.* **1988**, *176*, 329−334.
(7) Williams, P. A.; Day., D. H.; Langdon, M. J.; Phillips, G. O.; Nishinari, K. *Food Hydrocolloids* **1991**, *4*, 489−493.

(8) Dea, I. C. M.; Morris, E. R. *Am. Chem. Soc. Symp. Ser.* **1977**, *45*, 174−182.
(9) Goycoolea, F. M.; Richardson, R. K.; Morris, E. R.; Gidley, M. J. *Macromolecules* **1995**, *28*, 8308−8320.
(10) Annable, P.; Williams, P. A.; Nishinari, K. *Macromolecules* **1994**, *27*, 4204−4211.
(11) Nitta, Y.; Fang, Y.; Takemasa, M.; Nishinari, K. *Biomacromolecules* **2004**, *5*, 1206−1213.
(12) Nitta, Y.; Kim, B. S.; Nishinari, K. *Biomacromolecules* **2003**, *4*, 1654−1660.
(13) Ikeda, S.; Nitta, Y.; Kim, B. S.; Temsiripong, T.; Pongsawatmanit, R.; Nishinari, K. *Food Hydrocolloids* **2004**, *18*, 669−675.
(14) Reid, J. S. G.; Edwards, M.; Dea, I. C. M. In *Gums and Stabilisers for the Food Industry*; Phillips, G. O., Wedlock, D. J., Williams, P. A., Eds.; IRL Press: Oxford, 1988; Vol. 4, pp 391−398.
(15) Shirakawa, M.; Yamatoya, K.; Nishinari, K. *Food Hydrocolloids* **1998**, *12*, 25−28.
(16) Hayashi, T. *Annu. Rev. Plant Physiol. Plant Mol. Biol.* **1989**, *40*, 139−168.
(17) Glicksman, M. *Food Hydrocolloids*; Glicksman, M., Ed.; CRC Press: Boca Raton, FL, 1986; Vol. 3.
(18) Nishinari, K.; Yamatoya, K.; Shirakawa, M. In *Handbook of Hydrocolloids*; Phillips, G. O., Williams, P. A., Eds.; CRC Press: Boca Raton, FL, 2000; pp 247−267.
(19) Yoshimura, M.; Takaya, T.; Nishinari, K. *Food Hydrocolloids* **1999**, *13*, 101−111.
(20) York, W. S.; Vanhalbeek, H.; Darvill, A. G.; Albersheim, P. *Carbohydr. Res.* **1990**, *200*, 9−31.
(21) Whitcomb, P. J.; Macosko, C. W. *J. Rheol.* **1978**, *22*, 493−505.
(22) Jansson, P. E.; Kenne, L.; Lindberg, B. *Carbohydr. Res.* **1975**, *45*, 275−282.
(23) Melton, L. D.; Mindt, L.; Rees, D. A.; Sanderson, G. R. *Carbohydr. Res.* **1976**, *46*, 245−257.
(24) Cheetham, N. W. H.; Mashimba, E. N. M. *Carbohydr. Polym.* **1992**, *17*, 127−136.
(25) Holzwarth, G. *Biochemistry* **1976**, *15*, 4333−4339.
(26) Holzwarth, G.; Ogletree, J. *Carbohydr. Res.* **1979**, *76*, 277−280.
(27) Callet, F.; Milas, M.; Rinaudo, M. *Int. J. Biol. Macromol.* **1987**, *9*, 291−293.
(28) Shatwell, K. P.; Sutherland, I. W.; Dea, I. C. M.; Ross-Murphy, S. B. *Carbohydr. Res.* **1990**, *206*, 87−103.
(29) Smith, I. H.; Symes, K. C.; Lawson, C. J.; Morris, E. R. *Int. J. Biol. Macromol.* **1981**, *3*, 129−134.
(30) Fernandes, P. B.; Goncalves, M. P.; Doublier, J. L. *Carbohydr. Polym.* **1991**, *16*, 253−274.
(31) Kohyama, K.; Iida, H.; Nishinari, K. *Food Hydrocolloids* **1993**, *7*, 213−226.
(32) Goycoolea, F. M.; Richardson, R. K.; Morris, E. R.; Gidley, M. J. *Biopolymers* **1995**, *36*, 643−658.
(33) Morris, E. R. In *Biopolymer Mixtures*; Harding, S. E., Hill, S. E., Mitchell, J. R., Eds.; Nottingham University Press: Nottingham, U.K., 1995; pp 247−288.
(34) Paoletti, S.; Cesaro, A.; Delben, F. *Carbohydr. Res.* **1983**, *123*, 173−178.
(35) Viebke, C.; Piculell, L.; Nilsson, S. *Macromolecules* **1994**, *27*, 4160−4166.
(36) Rochas, C.; Rinaudo, M. *Biopolymers* **1980**, *19*, 1675−1687.
(37) Milas, M.; Shi, X.; Rinaudo, M. *Biopolymers* **1990**, *30*, 451−464.
(38) Norton, I. T.; Goodall, D. M.; Morris, E. R.; Rees, D. A. *J. Chem. Soc., Chem. Commun.* **1980**, 545−547.
(39) Kitamura, S.; Kuge, T.; Stokke, B. T. In *Gums and Stabilisers for the Food Industry*; Phillips, G. O., Wedlock, D. J., Williams, P. A., Eds.; IRL Press: Oxford, 1989; Vol. 5, pp 329−332.
(40) Kitamura, S.; Takeo, K.; Kuge, T.; Stokke, B. T. *Biopolymers* **1991**, *31*, 1243−1255.
(41) Bresolin, T. M. B.; Milas, M.; Rinaudo, M.; Ganter, J. *Int. J. Biol. Macromol.* **1998**, *23*, 263−275.
(42) Morris, E. R.; Rees, D. A.; Young, G.; Walkinshaw, M. D.; Darke, A. *J. Mol. Biol.* **1977**, *110*, 1−16.
(43) Paradossi, G.; Brant, D. A. *Macromolecules* **1982**, *15*, 874−879.
(44) Rinaudo, M.; Milas, M.; Lambert, F.; Vincendon, M. *Macromolecules* **1983**, *16*, 816−819.
(45) Tako, M.; Asato, A.; Nakamura, S. *Agric. Biol. Chem.* **1984**, *48*, 2995−3000.
(46) Foster, T. J.; Morris, E. R. In *Gums and Stabilisers for the Food Industry*; Phillips, G. O., Williams, P. A., Wedlock, D. J., Eds.; IRL Press: Oxford, 1994; Vol. 7, pp 281−289.
(47) Goycoolea, F. M.; Foster, T. J.; Richardson, R. K.; Morris, E. R.; Gidley, M. J. In *Gums and Stabilisers for the Food Industry*; Phillips, G. O., Williams, P. A., Wedlock, D. J., Eds.; IRL Press: Oxford, 1994; Vol. 7, pp 333−344.
(48) Cairns, P.; Miles, M. J.; Morris, V. J. *Nature* **1986**, *322*, 89−90.
(49) Chandrasekaran, R.; Radha, A. *Carbohydr. Polym.* **1997**, *32*, 201−208.
(50) Chandrasekaran, R.; Janaswamy, S.; Morris, V. J. *Carbohydr. Res.* **2003**, *338*, 2889−2898.
(51) Tako, M.; Nakamura, S. *Carbohydr. Res.* **1985**, *138*, 207−213.
(52) Richter, S.; Brand, T.; Berger, S. *Macromol. Rapid Commun.* **2005**, *26*, 548−553.

BM050734+